Annals of Physics 430 (2021) 168498

Contents lists available at ScienceDirect

Annals of Physics

journal homepage: www.elsevier.com/locate/aop

Quark stars in the Einstein–Gauss–Bonnet theory: A new branch of stellar configurations

Takol Tangphati [a,*], Anirudh Pradhan [b], Abdelghani Errehymy [c], Ayan Banerjee [d]

[a] Department of Physics, Faculty of Science, Chulalongkorn University, Bangkok 10330, Thailand
[b] Department of Mathematics, Institute of Applied Sciences and Humanities, GLA University, Mathura-281 406, Uttar Pradesh, India
[c] Laboratory of High Energy Physics and Condensed Matter (LPHEMaC), Department of Physics, Faculty of Sciences Aïn Chock, Hassan II University of Casablanca, B.P. 5366 Maarif, Casablanca 20100, Morocco
[d] Astrophysics Research Centre, School of Mathematics, Statistics and Computer Science, University of KwaZulu–Natal, Private Bag X54001, Durban 4000, South Africa

ARTICLE INFO

Article history:
Received 6 March 2021
Accepted 4 May 2021
Available online 11 May 2021

ABSTRACT

The observations of pulsars heavier than $2M_{\odot}$ have put strong constraints on the equation of state (EoS) above nuclear saturation density. For this reason, the internal structure of a neutron star which is strictly correlated with the EoS is an active area of investigation in theoretical astrophysics. Here, we investigate the possible sequels for the quark stars consisting of a homogeneous and unpaired charge-neutral 3-flavor interacting quark matter with $\mathcal{O}(m_s^4)$ corrections that accounts for the quark strong interactions. In particular, the quark stars (QSs) with a well-motivated quantum chromodynamics (QCD) EoS are presented in Einstein gravity with the Gauss–Bonnet (GB) combination of quadratic curvature terms. We analyze the dependence of the physical properties of these QSs on the Gauss–Bonnet coupling strength. In fact, the existence and stability of QSs depend on the effects of fourth-order corrections parameter (a_4) of the QCD perturbation. We also present and discuss the calculated results for mass–central mass density (M–ρ_c) relation and also the mass–radius (M–R) relation of QSs. Nevertheless, such deviations may be observable in future astrophysical probes.

* Corresponding author.
E-mail addresses: takoltang@gmail.com (T. Tangphati), pradhan.anirudh@gmail.com (A. Pradhan), abdelghani.errehymy@gmail.com (A. Errehymy), ayanbanerjeemath@gmail.com (A. Banerjee).

https://doi.org/10.1016/j.aop.2021.168498
0003-4916/

1. Introduction

The gravity theory with higher-curvature term, the so-called Lovelock theories have attracted considerable attention, as alternative theories beyond general relativity (GR). This theory was introduced originally by Lanczos [1], and rediscovered by David Lovelock [2,3] in the 1970s. The idea is that there exist theories containing precise higher order curvature invariants that actually modify Einstein's field equations while satisfying the Bianchi identities i.e. $\Delta^{\mu}T_{\mu\nu} = 0$ and the equations of motion contain only up to second order derivatives of the metric. Besides, the theory shares a number of additional nice properties including Einstein gravity that are not enjoyed by other more general higher curvature theories. Consequently, this theory can have stable, constant curvature vacua and the quantization of the linearized theory is free of ghosts (see Refs. [4,5])

Since, the polynomial form of the Lagrangian in Lovelock theories; the zeroth and first order terms correspond to the cosmological constant and the Einstein–Hilbert action, while the second order term is the Gauss–Bonnet (GB) Lagrangian, respectively. Thus, GB gravity (also referred to as the Einstein–Gauss–Bonnet (EGB) gravity) is a particular case of more general Lovelock gravity emerges as a low energy effective action of heterotic string theory [6–8]. Of course, the EGB gravity, which is under consideration in the current paper, the equations of gravitational fields are still of second order derivatives of the metric and hence avoiding the Ostrogradsky instability [9]. In the context of four dimensional physics, the GB term does not contribute to the gravitational field equations, and thus EGB and GR are equivalent in $4D$ space–time.

Nevertheless, the EGB gravity allows us to explore several conceptual issues of gravity that includes finding astrophysical solutions and investigating their properties. The well known spherically symmetric static black hole solutions of EGB theory were obtained by Boulware and Deser [7] and later several authors explored exact black hole solutions and their interesting properties in the literature [10–14]. In the same context the spherical gravitational collapse of inhomogeneous dust has been explored in [15–18], radius of photon spheres [19], regular black holes [20] were extensively analyzed. On the other hand, in [21] authors have found asymptotically flat wormhole geometries in the framework of EGB gravity and investigate the effects of the GB term. In addition, Ghosh [22] showed that noncommutative geometry inspired EGB black holes.

The pulsars or Neutron stars (NSs) are very compact remnants of stellar evolution that ended their lives in supernova explosions [23,24]. While the study of NSs, the composition and the properties of matter are largely unknown at low temperatures and high baryon number densities, especially at densities $\rho \gtrsim 3\rho_0$, where $\rho_0 = 2.8 \times 10^{14}$ g/cm^3 is the density of the symmetric nuclear matter at saturation. Depending on the density reached at the core of NSs, a phase transition might be expected in the core of a NSs. Thus one would expect that there is a phase transition from hadron matter to quark matter (QM). Inspired by this point of view, some authors raised the conception of quark stars which consists of self-bound strange quark matter (SQM). Moreover, the discoveries of radio pulsars and some other accretion-powered X-ray sources indicate that the existence of 2 $M_{\odot}$ [25,26] NSs put forward a strong constraint on the EoS of matter. Thus, the dynamical evolution of such violent events and the behavior of matter at ultrahigh densities and relatively low temperatures, are still an open question, directly related with NSs Physics. As a consequence of this, there are several models for EoS but only few of them are reliable to extract their bulk properties and reveal how matter behaves in their interior.

Within this scenario, people try to find approximate methods which incorporate the basic features of Quantum Chromodynamics (QCD). Among them the MIT-Bag Model has become very popular in the study of SQM in the background of GR and as well as modified gravity theories. Furthermore, it is well-known that quarks are not at all free particles as they stay confined and the mechanism behind quark confinement has been clarified in QCD. In such a manner, Chodos and co-workers [27] have portrayed that a strongly interacting particle may be characterized in a limited area of space under the fields action. They also argued that Bag constant B is a particularly restricted area containing constant energy density. This provides a reason for how the Bag constant can handle both the geometry of space–time and the energy–momentum tensor. By engaging outcomes in QCD and quark interactions inside the heavenly core, the so-called color-flavored Locked (CFL) EoS has been recently employed in acquiring models of compact stellar structures which approximate

realistic strange stars (SSs), pulsars and NSs to a generally agreeable degree [28,29]. In this way, the CFL EoS has also been used to survey the NSs surface tension. This survey exhibits that the surface tension is delicate to the Bag constant magnitude [30]. It was noticed that higher values of the Bag constant lead to celestial models with lower surface tensions and tangential pressures. Beside that M–R relation for NSs from observations can help us to constrain EoS models. Under such conditions, theoretical models predict different EoSs for baryonic matter at such extreme densities in NSs interior.

In fact, the inevitable softening of the EoS, due to the hyperonization makes the maximal mass limit significantly lower than $2M_{\odot}$ [31,32] for non-magnetic NSs. Motivated by the preceding discussion, we consider homogeneously confined matter inside the star with 3-flavor neutral charge and a fixed strange quark mass [33] in 5D EGB gravity. The coexistence of NSs and QSs has been proposed and discussed in detail in several papers, see for example [34–36]. Exact solutions to the field equations in the framework of EGB gravity have been already performed in some previous works [37,38]. We believe that our results can be of a certain interest because we compared our solutions with observational constraints from various pulsar measurements: J0348+0432 [26], J1903+0327 [39], EXO 1745-248 [40], 4U 1608-52 [41] and PSR J0437-4715 [42].

The paper is organized as follows: after a brief introduction in Section 1, we write down the equation of motion governing 5D EGB theory in Section 2. In the same section, we write down the equations describing the structure of the relativistic stars in EGB gravity. In Section 3 we review the structure equations describing QSs made of interacting quark matter. In next we discuss the numerical procedure that is used to solve the field equations in Section 4. Here, we present mass–radius curves that will give an insight to the stability of certain class of stellar configurations. The equations governing the QSs properties are explained in Section 5. Finally, we conclude our findings in Section 6.

2. Basic equations of EGB gravity

Here we recall the action of EGB theory. The action of GB gravity in D dimensional space–time can be written in the form of

$$\mathcal{I}_G = \frac{c^4}{16\pi G}\int d^D x\sqrt{-g}\,[R - 2\Lambda + \alpha\mathcal{L}_{\rm GB}] + \mathcal{S}_{\rm matter}, \tag{1}$$

where g denotes the determinant of the metric $g_{\mu\nu}$ and α is the GB coupling constant with dimension [length]^2. The Ricci scalar R provides the general relativistic part of the action. The EGB Lagrangian $\mathcal{L}_{\rm GB}$ is given by

$$\mathcal{L}_{\rm GB} = R^{\mu\nu\rho\sigma}R_{\mu\nu\rho\sigma} - 4R^{\mu\nu}R_{\mu\nu} + R^2. \tag{2}$$

We add also the matter action $\mathcal{S}_{\rm matter}$ which induces the energy–momentum tensor $T_{\mu\nu}$. If the above action, Eq. (1), is varied with respect to $g_{\mu\nu}$, one obtains the field equations

$$G_{\mu\nu} + \alpha H_{\mu\nu} = \frac{8\pi G}{c^4}T_{\mu\nu}\,, \quad \text{where} \quad T_{\mu\nu} = -\frac{2}{\sqrt{-g}}\frac{\delta\left(\sqrt{-g}\mathcal{S}_m\right)}{\delta g^{\mu\nu}}, \tag{3}$$

with $G_{\mu\nu}$ is the Einstein tensor and $H_{\mu\nu}$ is the contribution of the GB term with the following expression

$$\begin{aligned} G_{\mu\nu} &= R_{\mu\nu} - \frac{1}{2}R\,g_{\mu\nu}, \\ H_{\mu\nu} &= 2\Big(RR_{\mu\nu} - 2R_{\mu\sigma}R^{\sigma}{}_{\nu} - 2R_{\mu\sigma\nu\rho}R^{\sigma\rho} - R_{\mu\sigma\rho\delta}R^{\sigma\rho\delta}{}_{\nu}\Big) - \frac{1}{2}\,g_{\mu\nu}\,\mathcal{L}_{\rm GB}, \end{aligned} \tag{4}$$

where $R_{\mu\nu}$ is the Ricci tensor, R and $R_{\mu\sigma\nu\rho}$ are the Ricci scalar and the Riemann tensor, respectively. Additionally, GB term is total derivative in 4D space–time, and hence do not contribute to the field equations.

Here, we consider static spherically symmetric D-dimensional metric anstaz with two independent functions of radial coordinate, which is:

$$ds_D^2 = -e^{2\Phi(r)}c^2dt^2 + e^{2\Lambda(r)}dr^2 + r^2d\Omega_{D-2}^2, \tag{5}$$

where $d\Omega_{D-2}^2$ is the metric on the unit $(D-2)$-dimensional sphere and $\Phi(r)$ and $\Lambda(r)$ are functions of r, only. The energy–momentum tensor $T_{\mu\nu}$ is a perfect fluid matter source and describe the interior of a star, which in this study is written as

$$T_{\mu\nu} = (\epsilon + P)u_\nu u_\nu + Pg_{\nu\nu}, \tag{6}$$

where $P = P(r)$ is the isotropic pressure, $\epsilon = \epsilon(r)$ is the energy density of matter, and u_ν is the contravariant D-velocity. On using the metric (5) with stress tensor (6), the tt, rr and hydrostatic continuity equations (3) read:

$$\frac{2}{r}\frac{d\Lambda}{dr} = e^{2\Lambda}\left[\frac{2}{(D-2)}\frac{8\pi G}{c^4}\epsilon - \frac{1-e^{-2\Lambda}}{r^2}\left((D-3) + \frac{\alpha(D-5)(1-e^{-2\Lambda})}{r^2}\right)\right] \times \left[1 + \frac{2\alpha(1-e^{-2\Lambda})}{r^2}\right]^{-1}, \tag{7}$$

$$\frac{2}{r}\frac{d\Phi}{dr} = e^{2\Lambda}\left[\frac{2}{(D-2)}\frac{8\pi G}{c^4}P + \frac{1-e^{-2\Lambda}}{r^2}\left((D-3) + \frac{\alpha(D-5)(1-e^{-2\Lambda})}{r^2}\right)\right] \times \left[1 + \frac{2\alpha(1-e^{-2\Lambda})}{r^2}\right]^{-1}, \tag{8}$$

$$\frac{dP}{dr} = -(\epsilon + P)\frac{d\Phi}{dr}. \tag{9}$$

As usual, the asymptotic flatness imposes $\Phi(\infty) = \Lambda(\infty) = 0$ while the regularity at the center requires $\Lambda(0) = 0$. It is the purpose of this paper to obtain 5-dimensional ($5D$) spherically symmetric star solution for the EGB gravity.

At this point the gravitational mass within the sphere of radius r is defined by $e^{-2\Lambda} = 1 - \frac{2Gm(r)}{c^2r}$. Now, we are ready to write the Tolman–Oppenheimer–Volkoff (TOV) equations in a convenient form. Thus, combination of the conservation law equation (9) provides the following relation in five dimensions

$$\frac{dP}{dr} = -\frac{2G\epsilon(r)m(r)}{c^2r^2}\frac{\left[1 + \frac{P(r)}{\epsilon(r)}\right]\left[1 + \frac{4}{3}\frac{\pi r^3P(r)}{c^2m(r)}\right]}{\left[1 + \frac{4G\alpha m(r)}{c^2r^3}\right]\left[1 - \frac{2Gm(r)}{c^2r}\right]}. \tag{10}$$

We recover the standard TOV equation of GR when $\alpha \to 0$. Replacing the last equality in Eq. (7), we obtain the gravitational mass:

$$m'(r) = \frac{-3c^2r^3m(r) + 12\alpha Gm(r)^2 + 8\pi r^6\epsilon(r)}{3\left(c^2r^4 + 4\alpha Grm(r)\right)}, \tag{11}$$

using the initial condition $m(0) = 0$, here the prime $(')$ denotes differentiation with respect to r. Then we use the dimensionless variables $P(r) = \epsilon_0\bar{P}(r)$ and $\epsilon(r) = \epsilon_0\bar{\epsilon}(r)$ and $m(r) = M_\odot\bar{M}(r)$, with $\epsilon_0 = 1\,\mathrm{MeV/fm^3}$. As a result, the above two equations become

$$\frac{d\bar{P}(r)}{dr} = -\frac{2G\bar{\epsilon}(r)M_\odot\bar{M}(r)}{c^2r^2}\frac{\left[1 + \frac{\bar{P}(r)}{\bar{\epsilon}(r)}\right]\left[1 + \frac{4}{3}\frac{\pi r^3\epsilon_0\bar{P}(r)}{c^2M_\odot\bar{M}(r)}\right]}{\left[1 + \frac{4G\alpha M_\odot\bar{M}(r)}{c^2r^3}\right]\left[1 - \frac{2GM_\odot\bar{M}(r)}{c^2r}\right]} = -\frac{2c_1\bar{\epsilon}(r)\bar{M}(r)}{r^2}\frac{\left[1 + \frac{\bar{P}(r)}{\bar{\epsilon}(r)}\right]\left[1 + \frac{c_2r^3\bar{P}(r)}{3\bar{M}(r)}\right]}{\left[1 + \frac{4c_1\alpha\bar{M}(r)}{r^3}\right]\left[1 - \frac{2c_1\bar{M}(r)}{r}\right]}, \tag{12}$$

and

$$M_\odot \frac{d\bar{M}(r)}{dr} = \frac{-3c^2r^3M_\odot\bar{M}(r) + 12\alpha G M_\odot^2\bar{M}(r)^2 + 8\pi r^6\epsilon_0\bar{\epsilon}(r)}{3(c^2r^4 + 4\alpha G r M_\odot\bar{M}(r))}$$
$$\frac{d\bar{M}(r)}{dr} = \frac{-3r^3\bar{M}(r) + 12c_1\alpha\bar{M}(r)^2 + 2c_2r^6\bar{\epsilon}(r)}{3(r^4 + 4c_1\alpha r\bar{M}(r))}, \tag{13}$$

where $c_1 \equiv \frac{GM_\odot}{c^2} = 1.474$ km and $c_2 \equiv \frac{4\pi\epsilon_0}{M_\odot c^2} = 1.125 \times 10^{-5}$ km^{-3}. Eqs. (12) and (13) can be solved numerically for a given EoS. For the sake of simplicity, one needs to add an EoS of the form $P = P(\epsilon)$, which we will discuss in the next section.

3. Interacting quark matter equation of state

The composition and structure of compact stars depend on the nature of strong interaction. It is natural to speculate that when nuclear matter is compressed to a sufficiently high density then the nucleon cores substantially overlap. The overlapping core of nucleons undergoes a new phase of matter, in which quarks are the relevant degrees of freedom. Earlier this was pointed out by Ivanenko & Kurdgelaidze [43] as a possible existence of a *quarkian core* in very massive stars. Thus, one expects the core of the NSs to be composed of different phases of exotic matter with large strangeness fraction such as hyperon matter, Bose–Einstein condensates of strange mesons or quark matter. The so called Bodmer–Witten hypothesis on the absolute stability of strange quark matter (see [44,45] for review) suggests that there exists a particular class of compact stars, so called strange stars [46,47], where the core consists of equal amounts of *up, down and strange* quarks, and a small number of electrons to attain the charge neutrality.

There have been some models used to approach the strange matter (SM) hypothesis; the MIT-Bag Model is one of the most successful phenomenological models for quark confinement developed at the Massachusetts Institute of Technology in Cambridge (USA) in 1974. In this model, hadrons are considered as extended static objects localized in space in which each quark moves freely in a spherically symmetric well of infinity depth (bag). The simplicity of this model makes it attractive and convenient for calculating various hadronic properties. Beside that several other works have also predicted the existence of a large variety of color superconducting states of quark matter at ultra-high densities, see Refs. [48–51] for details.

In this paper we would like to have a quark matter model that could consist of homogeneous and unpaired charge neutral 3-flavor interacting quark matter. For simplicity, we describe this phase using the simple thermodynamic Bag model EoS [52] with $\mathcal{O}(m_s^4)$ corrections. These corrections account for the moderately heavy strange quark. In this context, QSs models have been successfully proposed in [34,53] and discuss the modes of oscillation. Finally, the interacting quark EoS reads

$$P = \frac{1}{3}(\epsilon - 4B) - \frac{m_s^2}{3\pi}\sqrt{\frac{\epsilon - B}{a_4}} + \frac{m_s^4}{12\pi^2}\left[1 - \frac{1}{a_4} + 3\ln\left(\frac{8\pi}{3m_s^2}\sqrt{\frac{\epsilon - B}{a_4}}\right)\right]. \tag{14}$$

Here ϵ represents the energy density of homogeneously distributed quark matter, B stands for the Bag constant and m_s indicates the strange mass of the quark, while a_4 is a parameter resulting from the QCD corrections on the pressure of the Fermi sea without quarks, which is linked with the maximum mass of the stellar structure around $\sim 2M_\odot$ at $a_4 \approx 0.7$ as proposed in [54]. As an evidence heavy hybrid stars ($M \sim 2M_\odot$) while still ensuring that the nuclear matter to quark matter phase transition occurs above nuclear saturation density for $a_4 \approx 0.7$ [52]. Such dependence also assures the possibility to mimic the mass–radius behavior of nucleonic stars over a wide range of masses.

Now, in order to determine the maximum masses M and their corresponding radii R for QSs, we have to solve the system of TOV equations (12) and (13) for homogeneous EoS in (14). We now set out the boundary conditions $P(r_0) = P_c$ and $M(R) = M$, and integrate Eq. (12) outwards to a certain radius $r = R$ where fluid pressure P vanishes i.e. $P(R) = 0$. This leads to the QS radius R and mass $M = m(R)$. Note that we set a very small positive number with initial radius $r_0 = 10^{-5}$ and mass $m(r_0) = 10^{-30}$ rather than zero to avoid the discontinuities that appear in the denominators.

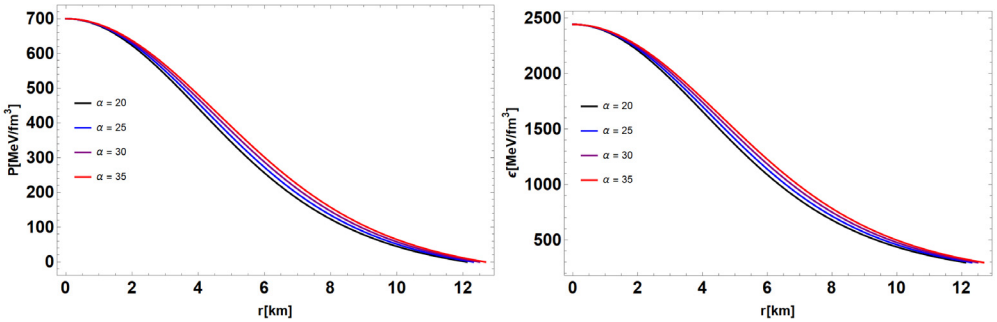

Fig. 1. The variation of pressure (left panel) and energy density (right panel) with radius for the interacting EoS. Our choices for pressure at the core is $P(r_0) = 700$ MeV/fm^3, $B = 70$ MeV/fm^3, $a_4 = 0.7$ and the variation of α from 20 to 35 km^2.

Here, we adopt the unit conversion 1 fm $=$ 197.3 MeV to synchronize each term given in Eq. (14). Introducing this conversion, we find MeV^4 $=$ 197.3^{-3} MeV fm^{-3}. Finally, Eq. (14) reads

$$P = \frac{1}{3}(\epsilon - 4B) - \frac{1}{3\pi}\sqrt{\frac{1}{197.3^3}}\, m_s^2 \sqrt{\frac{\epsilon - B}{a_4}} + \frac{1}{12\pi^2}\frac{m_s^4}{197.3^3}\left[1 - \frac{1}{a_4} + 3\ln\left(\frac{8\pi}{3m_s^2}\sqrt{197.3^3}\sqrt{\frac{\epsilon - B}{a_4}}\right)\right]. \tag{15}$$

Now, in order to analyze the behavior of the quark matter with $\mathcal{O}(m_s^4)$ corrections, we show how the pressure and energy density are distributed with the help of a median value of the Bag constant B containing within the range $57 \leq B \leq 92$ MeV/fm^3, specifically around $B \sim 70$ MeV/fm^3. This bound applied to the Bag constant is established via the stability condition against iron nuclei for 2-flavor and 3-flavor quark matter as suggested by the authors [55]. For our calculations, we set the strange quark mass m_s to be 100 MeV [56], and varying the parameter a_4 and the Bag constant B from $a_4 = 0.1$ to 0.9 and $B = 57$ to 92 MeV/fm^3, respectively.

We plot diagrams related to the pressure and density with respect to the radial coordinate r in Fig. 1. As we can see that both quantities viz., the pressure and density are regular at the center of the star and decrease monotonically towards the stellar surface. Moreover, we observe that when the GB coupling constant α increases from 20 to 35 km^2 by setting the parameter a_4 and the Bag constant B to 0.7 and 70 MeV/fm^3 respectively, leading to a higher pressure and density at every point of the stellar interior.

4. Numerical model and analysis of mass–radius relation

In the previous section, we describe the EoS (15) that needs to supplement the TOV equations in order to solve them and find the mass–radius relationship. To get the structure of a star, we have to integrate from the origin with the initial conditions $m(0) = 0$ and a particular value of central pressure, $P_c = P(r_0) = 700$ MeV/fm^3. Using these initial values of the pressure and mass-function one integrates Eqs. (12) and (13) until the value of the pressure becomes zero or drops to a very small value. Note that for the value of r at where $P = 0$ is identified as the radius R, and $m(r = R) = M$ is the total 'mass' of the star. We obtain a sequence of equilibrium configurations by varying the values of α and a_4, and record the mass and the radius for each case, respectively. The mass is measured in the solar mass unit $M_\odot$, radius in km, while energy density, pressure and bag constant B are in unit of MeV/fm^3. In this work the values of parameters were being found in the range $0 < a_4 < 1$ and $57 < B < 92$ MeV/fm^3 [44].

Since, the maximum mass of NS is still an open question, we focus on the mass–radius (M–R) relation depending on the choice of various parameters. Fig. 2 displays the M–R relation for QSs with two different values of the bag constant B and various values of the GB coupling α. We stress that recent works [57,58] have exploited the increasing availability of high-quality data to pindown

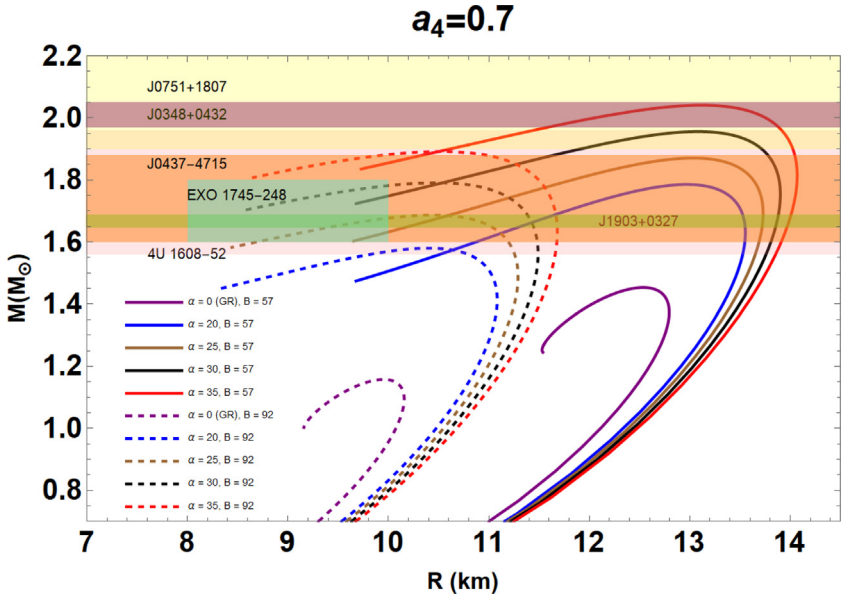

Fig. 2. Mass–radius relation where the bag constant is set to $B = 92$ MeV/fm^3 (dashed line) and $B = 57$ MeV/fm^3 (solid line). The parameters $a_4 = 0.7$ and the GB coupling α take several values. The horizontal bands show the observational constraints from various pulsar measurements: J0348+0432 [26], J1903+0327 [39], EXO 1745-248 [40], 4U 1608-52 [41] and PSR J0437-4715 [42].

masses and radii of selected stellar systems. Here we include some particular pulsars like PSR J0348+0432 [26] about $2.01 \pm 0.04 M_\odot$, PSR J1903+0327 [39] about $1.667 \pm 0.021\, M_\odot$, EXO 1745-248 [40] about $M = 1.7 \pm 0.1\, M_\odot$, 4U 1608-52 [41] about $1.74 \pm 0.14\, M_\odot$ and PSR J0437-4715 [42] about $1.76 \pm 0.20 M_\odot$ to put theoretical constraints on the properties of the maximum-mass NSs that can be achieved by extended theories of gravity as EGB gravity and then compare the solution with GR i.e. $\alpha = 0$. Nevertheless, one should note that models and data are still subject to detailed analysis.

Concerning the $M-R$ sequences in Fig. 2 for two different values of Bag constant $B = 92$ MeV/fm^3 (dashed line) and $B = 57$ MeV/fm^3 (solid line) one can easily see that for smallest value the bag parameter shows a good agreement with the astrophysical data. Interestingly, we found that the maximum mass of QS reaches the $2M_\odot$ limit for $B = 57\,\text{MeV/fm}^3$ when $\alpha = 35$ km^2 and $a_4 = 0.7$. Significantly these solutions fall in the radius of a neutron star must be in the range of $R \lesssim (11 \sim 14)$ km [59]. While for specific value of $B = 92$ MeV/fm^3, we obtain values of the mass and radius in agreement with the ones reported in Gourgoulhon et al. [60] for non-rotating QSs. Considering the same EoS, reported in [34], the maximum mass was achieved for lowest value of the Bag parameter $B = 57\,\text{MeV/fm}^3$. In our model, we have a similar trend but the mass–radius measurements are larger than the Einstein gravity (see Fig. 2 in [34] and references therein). This is because the presence of α term in EGB gravity which leads to the maximum mass of the QSs for positive values of α. The results of numerical analysis are presented in Table 1 for each α and the given EoS model we consider in this work.

Next, we investigate the effect of the parameter a_4 in Fig. 3, where the M–R relations are reported for two values of the parameter α and different values of B. In this figure we also show, represented by the various horizontal stripes, some observed values for the mass of the massive NSs ever detected, as of Fig. 2. We can see how both the mass and the radius change with increasing the value of a_4. So this result strongly suggests that the a_4 parameter is highly relevant in determining the maximum mass of a NS with an interacting quark EoS. The curve has a maximum mass

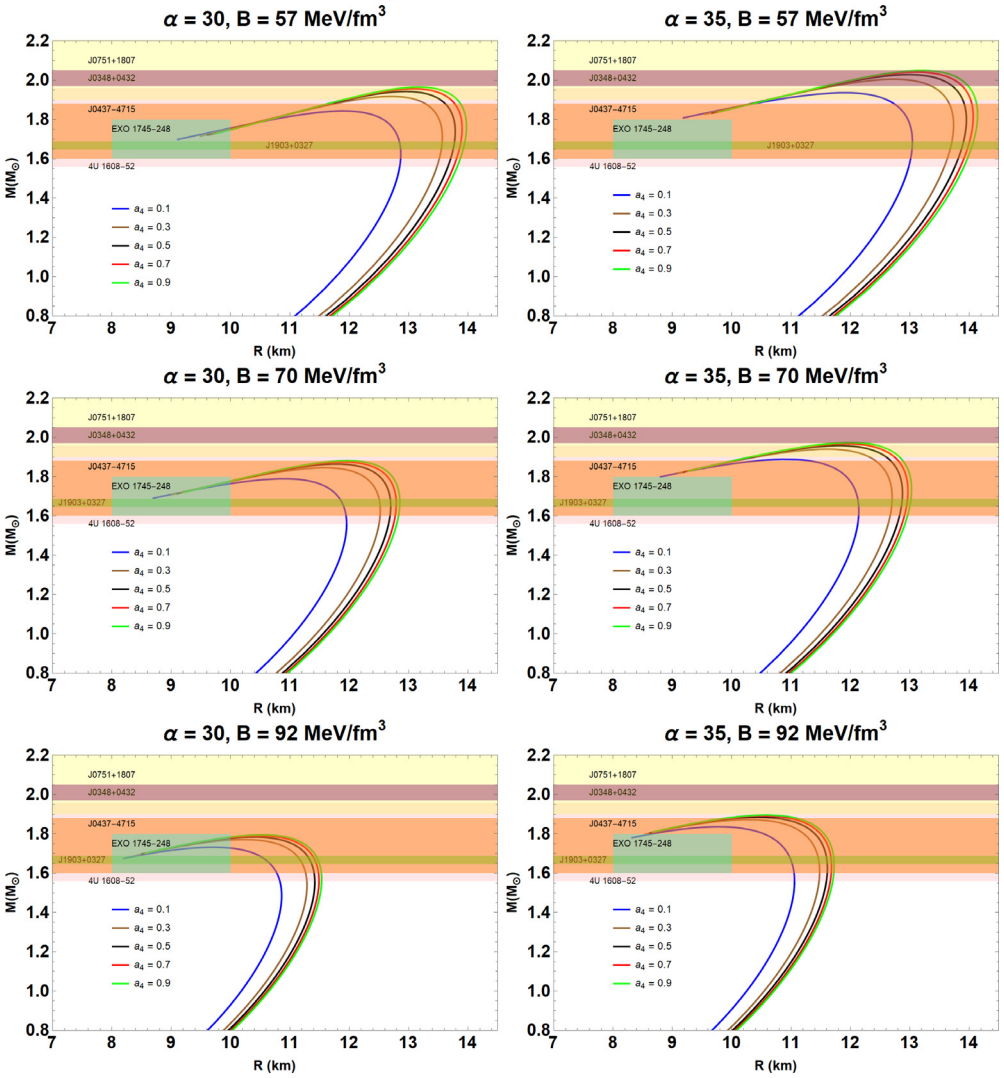

Fig. 3. The mass–radius diagram for an interacting quark EoS for (a) B = 57, (b) B = 70 and (c) B = 92 in MeV/fm^3, respectively. Here we set GB coupling constant $\alpha = 30$ and $\alpha = 35$ in km^2 for different values of a_4.

$M_{\max} = 2.08\ M_\odot$ at radius $R_{\max} = 14$ km assuming $a_4 = 0.9$. Thus, it is possible to restrict the EoS for a fixed value of the Bag parameter and coupling constant. In the end, a profile of solutions that covers the full range of values for α and B is presented in Fig. 4. For comparison, we see that for less interacting quarks the mass and radius are much larger compared to highly interacting quarks and do not even reach the $2M_\odot$ constraint. We note here that the maximum mass of a QSs can be larger than that in GR when the parameter α in EGB gravity is positive.

5. Structural properties of strange stars

For completeness, we would also like to explore the physical properties in the interior of the fluid sphere.

Table 1
We summarize the parameters of the QSs using various values of the 5*D* EGB coupling constant, α. We show the maximum mass of the stars M in a unit of the solar mass $M_\odot$ with their radius R in km and the central energy density ϵ_c in MeV/fm^3.

Quark Stars with $B = 57$ and $a_4 = 0.7$				
α (km^2)	$M_{\max}$ ($M_\odot$)	R (km)	ϵ_c (MeV/fm^3)	$B_{\rm bind}^{\max}$ ($M_{\max}$)
20	1.79	12.97	2.69×10^3	0.141
25	1.87	13.03	3.00×10^3	0.148
30	1.96	13.08	3.30×10^3	0.154
35	2.04	13.12	3.60×10^3	0.162
Quark Stars with $B = 92$ and $a_4 = 0.7$				
α (km^2)	$M_{\max}$ ($M_\odot$)	R (km)	ϵ_c (MeV/fm^3)	$B_{\rm bind}^{\max}$ ($M_{\max}$)
20	1.58	10.40	5.26×10^3	0.157
25	1.69	10.44	6.17×10^3	0.169
30	1.79	10.49	7.08×10^3	0.179
35	1.89	10.53	7.98×10^3	0.191

5.1. The stability criterion and the adiabatic indices

In the light of above considerations, Fig. 5 shows the stellar mass M, in solar masses $M_\odot$, against the central energy density ϵ_c for different values of GB constant α and a_4, respectively. We use central energy densities in the range $500 \leq \epsilon_c \leq 4000\,\text{MeV/fm}^3$. This correspondence means that $(M_{\max}, R_{M_{\max}})$ is a boundary separating the stable configuration region indicated by $\frac{\partial M(\epsilon_c)}{\partial \epsilon_c} > 0$ from the unstable one indicated by $\frac{\partial M(\epsilon_c)}{\partial \epsilon_c} < 0$. But this is a necessary condition but not sufficient. The solution branch, we consider in this work coincides with the GR solution [34] at low densities where the differences between EGB and GR are almost indistinguishable. But the situation changes when we increase the central densities. More specifically, depending on the central densities the maximum mass is larger than the corresponding values in GR. From Fig. 5, it is observed that the stellar mass increases with the central density in all cases except GR. It is also interesting to mention that, these solutions are then stable up to the point where the condition $\frac{\partial M(\epsilon_c)}{\partial \epsilon_c} > 0$. We have thus demonstrated the stability of compact stars in EGB gravity for all chosen values of the parameter $\alpha > 0$.

Another important criterion for a strange quark celestial structure linked to the thermodynamic quantity dubbed the adiabatic index which is a basic ingredient of the instability criterion. This adiabatic index is examined through the dynamic theory of infinitesimal radial and adiabatic oscillations of relativistic celestial structures which was first suggested by Chandrasekhar [61]. We now turn our attention to the stability of compact objects which can be analyzed by studying the adiabatic index of the astrophysical system. As another application of the adiabatic index represents the stiffness of the EoS for a given density profile, as pointed out by Harrison & Haensel et al. [62,63]. The final formula of the adiabatic index can be expressed mathematically as follows

$$\gamma \equiv \frac{P+\epsilon}{P}\left(\frac{dP}{d\epsilon}\right)_S, \tag{16}$$

while the subscript S represents such a derivation is carried out at constant specific entropy and the term in parentheses describes the velocity of sound in units of velocity of light. To demonstrate the adiabatic index that covers four different values of the GB coupling constant α for $B = 70\,\text{MeV/fm}^3$ and $a_4 = 0.7$, we show in Fig. 6 (left). It is well-known that the adiabatic index ought to surpass 4/3 in a stable polytropic stellar configuration by a quantity that relies upon that ratio ϵ/P at the core of the spherical body [64]. Additionally, the value of this ratio lies between 2 to 4 for the EoS related to neutron star matter [62]. In this regard, from the numerical scheme, we can note that throughout the astrophysical distribution, the adiabatic index is greater than 4/3 and therefore the stellar model

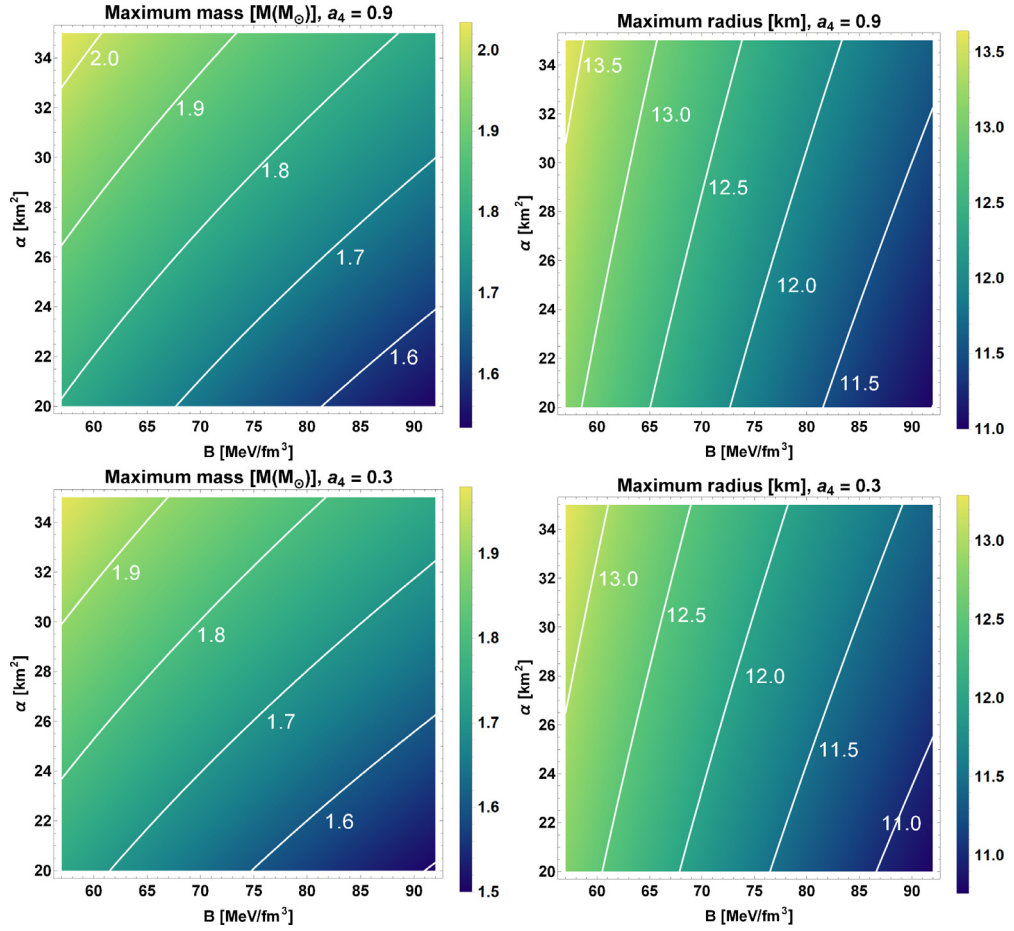

Fig. 4. Maximum masses and their corresponding radii for the full range of values of $20 \leq \alpha \leq 35$ km^2 and $57 \leq B \leq 92$ MeV/fm^3. We choose a particular value of the fourth-order-corrected parameter $a_4 = 0.9$ and 0.3, respectively.

represents a stable configuration against the radial adiabatic infinitesimal perturbations. On the other hand, for the GR case ($\alpha = 0$) we note that the stability of the configurations is also satisfied. Also, it should be mentioned here that when the values of γ increase, the values of the pressure gradually increase with a given increase in energy density.

5.2. Compactness and binding energy

In the context of compact objects an important source of information is the gravitational redshift [62] and defined by

$$Z_{\text{surf}} = \left(1 - r_g/R\right)^{-1/2} - 1, \tag{17}$$

which is produced by the photons emitted radially outward from the surface of a gravitational mass M. In (17) the $r_g = 2GM/c^2$ and R is the radius of the star. Since, compactness $2MG/Rc^2$ leads to the redshift value for the given EoS (14). We show the *compactness* parameter for particular values of the Bag parameter $B = 57$ and 92 MeV/fm^3 with different GB coupling constant α in Fig. 6. We

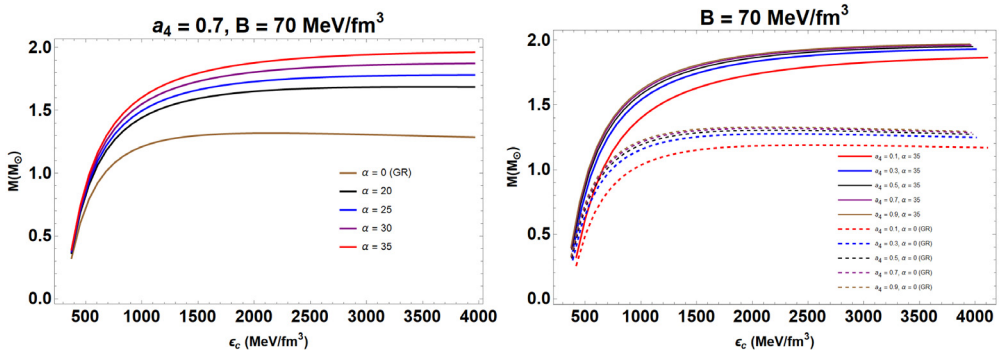

Fig. 5. Gravitational mass is plotted against the central density for compact stars modeled by the interacting EoS. We use central energy densities in the range $500 \leq \rho_c \leq 4000\,\mathrm{MeV/fm^3}$. Different values of α and a_4 are considered for $B = 70\,\mathrm{MeV/fm^3}$.

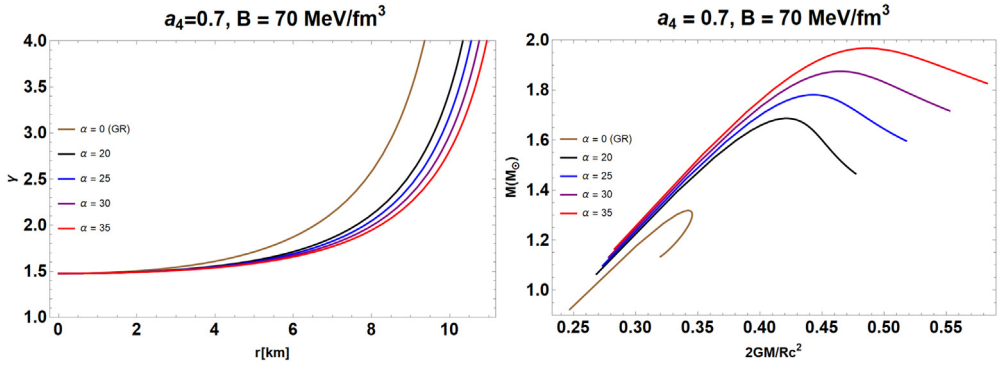

Fig. 6. The left panel shows the behavior of the adiabatic index γ. In the right panel mass of the star, normalized in solar masses $M_\odot$, versus the $2GM/c^2R$ (compactness). Four different values of α are considered for $B = 70\,\mathrm{MeV/fm^3}$ and $a_4 = 0.7$.

have seen in Fig. 6 that the trend of stellar compactness lies in the range of $0.5 < r_g/R < 0.6$ for some positive values of α. For the corresponding solution in GR, this value lies in the range of $0.3 < r_g/R < 3.5$. In other words in some cases EGB leads to more compact stars compared to GR.

In [65] authors have pointed out a universal relation between the total binding energy and the stellar mass of the NS, which yield

$$|E_t| \approx 0.084 \left(\frac{M}{M_\odot}\right)^2 M_\odot. \tag{18}$$

Note that the above expression is potentially applicable in determining the mass of NS through the binding energy. Later this formula was improved by Lattimer and Prakash [66]. Through the definition which turns out to be

$$\frac{B_{\mathrm{bind}}}{M} \simeq \frac{0.298\,\beta}{1 - 0.25\beta}. \tag{19}$$

where $\beta = r_g/R$ is the compactness parameter and the expression is radius dependent. The binding energy is explored for two different values of the bag constant and the interacting parameter $a_4 = 0.7$. It is evident from the last column of Table 1 that the binding energy i.e. $B_{\mathrm{bind}} = B_{\mathrm{bind}}^{\mathrm{max}}$ is higher for the larger bag parameter B.

6. Conclusions and astrophysical implications

In this article, we tried to carry out an analysis on static spherically symmetric solutions assuming an interacting EoS in the higher-curvature gravity theory, namely, Einstein–Gauss–Bonnet (EGB) gravity. Furthermore, we discuss the physical features of the EGB model on theoretical and observational grounds, identifying the role of free parameters which EGB differs significantly from standard GR. Since the EoS in (14) reduces to the MIT bag model if the quark mass (m_s) is zero. The coefficient a_4 comes from the QCD corrections on the pressure of the quark-free Fermi sea; plays an important role in determining the mass–radius relations. We take into account the cases for the influence of strong interactions when the coefficient a_4 lies between $0 < a_4 < 1$. In particular, the typical value of $a_4 = 1$ leads to free noninteracting quarks. Our considerations show that considerable increasing of mass can be achieved adopting the higher values of a_4. This effect can be seen clearly from Fig. 3, QS models with the maximum value of $a_4 = 0.9$ mostly produce maximum masses that seem to meet the PSR J0348+0432 two-solar-mass criterion, for $\alpha = 35$ km^2 and $B = 57$ MeV/fm^3.

Concerning the M–R diagram (see Fig. 2) resulting from the two different values of the Bag constant B, it is clear that the maximum mass of the solution exists for lower values of B. In the case of interacting EoS it turns out that QSs with masses larger than $2M_\odot$ are allowed in EGB for increasing value of $\alpha > 0$. We also found that the maximum mass of a QS can be much larger than that in GR when the parameter α in EGB gravity is positive. Also, we compare the results obtained from high precision measurements of the NSs maximal mass near the Galactic center to put a strong constraint on model parameters. In particular, we showed that the obtained maximum mass of QSs in 5D EGB gravity can cover most of the measured masses of pulsars and NSs.

Next, we addressed the issue of the static stability criterion [67] and studied the stability of QSs in EGB gravity. The condition $\frac{\partial M(\epsilon_c)}{\partial \epsilon_c} \lesseqgtr 0$ has been used to determine the regions constituted by stable or unstable against radial perturbations. Our results imply that the maximum mass increases simply monotonically with increasing ϵ_c values of EGB in compact stars, where we see deviations from GR (see Fig. 6). But, these conditions are necessary but not sufficient to recognize regions corresponding to stable and unstable stars. We have further investigated the adiabatic index γ, compactness and binding energy for the analysis of structure of QSs in modified gravity. As expected by increasing α the deviation between GR and EGB increases. It is interesting that for increasing value of α, EGB leads to more compact stars compared to standard GR counterparts. Finally, our concluding remark is that the behavior of compact quark stars in EGB gravity is sensitive depending on the choice of corrections parameter (a_4) and GB constant α.

CRediT authorship contribution statement

Takol Tangphati: Ideas, Formulation and writing- original draft preparation. **Anirudh Pradhan:** Application of mathematical formulation and computation. **Abdelghani Errehymy:** Writing - reviewing and validation. **Ayan Banerjee:** Writing - reviewing & editing.

Declaration of competing interest

The authors declare that they have no known competing financial interests or personal relationships that could have appeared to influence the work reported in this paper.

Acknowledgments

We wish to thank the anonymous reviewer for useful suggestions. TT would like to thank the financial support from the Science Achievement Scholarship of Thailand (SAST).

References

[1] C. Lanczos, Annals Math. 39 (1938) 842.
[2] D. Lovelock, J. Math. Phys. 12 (1971) 498.

[3] D. Lovelock, J. Math. Phys. 13 (1972) 874.
[4] B. Zwiebach, Phys. Lett. B 156 (1985) 315.
[5] B. Zumino, Phys. Rep. 137 (1986) 109.
[6] D.L. Wiltshire, Phys. Lett. B 169 (1986) 36.
[7] D.G. Boulware, S. Deser, Phys. Rev. Lett. 55 (1985) 2656.
[8] J.T. Wheeler, Nuclear Phys. B 268 (1986) 737.
[9] R.P. Woodard, Scholarpedia 10 (2015) 32243.
[10] S.G. Ghosh, M. Amir, S.D. Maharaj, Eur. Phys. J. C 77 (2017) 530.
[11] D. Rubiera-Garcia, Phys. Rev. D 91 (2015) 064065.
[12] A. Giacomini, J. Oliva, A. Vera, Phys. Rev. D 91 (2015) 104033.
[13] L. Aranguiz, X.M. Kuang, O. Miskovic, Phys. Rev. D 93 (2016) 064039.
[14] W. Xu, J. Wang, X.h. Meng, Phys. Lett. B 742 (2015) 225.
[15] S. Jhingan, S.G. Ghosh, Phys. Rev. D 81 (2010) 024010.
[16] H. Maeda, Phys. Rev. D 73 (2006) 104004.
[17] K. Zhou, Z.Y. Yang, D.C. Zou, R.H. Yue, Modern Phys. Lett. A 26 (2011) 2135.
[18] G. Abbas, M. Zubair, Modern Phys. Lett. A 30 (2015) 1550038.
[19] E. Gallo, J.R. Villanueva, Phys. Rev. D 92 (2015) 064048.
[20] S.G. Ghosh, D.V. Singh, S.D. Maharaj, Phys. Rev. D 97 (2018) 104050.
[21] H. Maeda, M. Nozawa, Phys. Rev. D 78 (2008) 024005.
[22] S.G. Ghosh, Classical Quantum Gravity 35 (2018) 085008.
[23] S.E. Woosley, A. Heger, T.A. Weaver, Rev. Modern Phys. 74 (2002) 1015.
[24] A. Heger, C.L. Fryer, S.E. Woosley, N. Langer, D.H. Hartmann, Astrophys. J. 591 (2003) 288.
[25] P. Demorest, T. Pennucci, S. Ransom, M. Roberts, J. Hessels, Nature 467 (2010) 1081.
[26] J. Antoniadis, P.C.C. Freire, N. Wex, et al., Science 340 (2013) 6131.
[27] A. Chodos, R.L. Jaffe, K. Johnson, C.B. Thorn, Phys. Rev. D 10 (1974) 2599.
[28] S. Thirukkanesh, A.A. Kaisavelu, M. Govender, Eur. Phys. J. C 80 (2020) 214.
[29] Ksh.N. Singh, A. Banerjee, S.K. Maurya, F. Rahaman, A. Pradhan, 2020, arXiv:2007.00455.
[30] R.S. Bogadi, M. Govender, S. Moyo, Phys. Rev. D 102 (2020) 043026.
[31] I. Vidana, A. Polls, A. Ramos, L. Engvik, M. Hjorth-Jensen, Phys. Rev. C 62 (2000) 035801.
[32] S. Weissenborn, D. Chatterjee, J. Schaffner-Bielich, Nuclear Phys. A 881 (2012) 62.
[33] J. Asbell, P. Jaikumar, J. Phys. Conf. Ser. 861 (2017) 012029.
[34] E.A. Becerra-Vergara, S. Mojica, F.D. Lora-Clavijo, A. Cruz-Osorio, Phys. Rev. D 100 (2019) 103006.
[35] A. Banerjee, T. Tangphati, D. Samart, P. Channuie, Astrophys. J. 906 (2021) 114.
[36] G. Panotopoulos, T. Tangphati, A. Banerjee, M.K. Jasim, arXiv:2104.00590 [gr-qc].
[37] S. Hansraj, B. Chilambwe, S.D. Maharaj, Eur. Phys. J. C 75 (2015) 277.
[38] S.D. Maharaj, B. Chilambwe, S. Hansraj, Phys. Rev. D 91 (2015) 084049.
[39] P.C.C. Freire, C.G. Bassa, N. Wex, et al., Mon. Not. R. Astron. Soc. 412 (2011) 2763.
[40] F. Ozel, T. Guver, D. Psaltis, Astrophys. J. 693 (2009) 1775.
[41] T. Guver, F. Ozel, A. Cabrera-Lavers, P. Wroblewski, Astrophys. J. 712 (2010) 964.
[42] J.P.W. Verbiest, M. Bailes, W. van Straten, G.B. Hobbs, R.T. Edwards, R.N. Manchester, N.D.R. Bhat, J.M. Sarkissian, B.A. Jacoby, S.R. Kulkarni, Astrophys. J. 679 (2008) 675.
[43] D. Ivanenko, D.F. Kurdgelaidze, Astrofizika 1 (1965) 479.
[44] E. Witten, Phys. Rev. D 30 (1984) 272.
[45] A.R. Bodmer, Phys. Rev. D 4 (1971) 1601.
[46] P. Haensel, J.L. Zdunik, R. Schaeffer, Astron. Astrophys. 160 (1986) 121.
[47] C. Alcock, E. Farhi, A. Olinto, Astrophys. J. 310 (1986) 261.
[48] A. Banerjee, K.N. Singh, arXiv:2005.04028 [gr-qc].
[49] G. Lugones, J.E. Horvath, Astron. Astrophys. 403 (2003) 173.
[50] R.S. Bogadi, M. Govender, S. Moyo, Phys. Rev. D 102 (2020) 043026.
[51] M. Matsuzaki, E. Kobayashi, J. Phys. G 34 (2007) 1621.
[52] M. Alford, M. Braby, M. Paris, S. Reddy, Astrophys. J. 629 (2005) 969.
[53] C.V. Flores, Z.B. Hall, P. Jaikumar, Phys. Rev. C 96 (2017) 065803.
[54] E.S. Fraga, R.D. Pisarski, J. Schaffner-Bielich, Phys. Rev. D 63 (2001) 121702.
[55] D. Blaschke, N. Chamel, Astrophys. Space Sci. Libr. 457 (2018) 337.
[56] J. Beringer, et al., Phys. Rev. D 86 (2012) 010001.
[57] F. Ozel, D. Psaltis, Phys. Rev. D 80 (2009) 103003.
[58] F. Ozel, G. Baym, T. Guver, Phys. Rev. D 82 (2010) 101301.
[59] A.W. Steiner, J.M. Lattimer, E.F. Brown, Astrophys. J. 722 (2010) 33.
[60] E. Gourgoulhon, P. Haensel, R. Livine, et al., Astron. Astrophys. 349 (1999) 851.
[61] S. Chandrasekhar, Phys. Rev. Lett. 12 (1964) 114; S. Chandrasekhar, ApJ. 140 (1964) 417.
[62] P. Haensel, A.Y. Potekhin, D.G. Yakovlev, Neutron Stars 1: Equation of State and Structure, Springer-Verlag, New York, 2007.
[63] B.K. Harrison, et al., Gravitational Theory and Gravitational Collapse, University of Chicago Press, Chicago, 1966.
[64] E.N. Glass, A. Harpaz, Mon. Not. R. Astron. Soc. 202 (1983) 1.
[65] J.M. Lattimer, A. Yahil, Astrophys. J. 340 (1989) 426.
[66] J.M. Lattimer, M. Prakash, Astrophys. J. 550 (2001) 426.
[67] B.K. Harrison, K.S. Thorne, M. Wakano, J.A. Wheeler, Gravitation Theory and Gravitational Collapse, University of Chicago Press, Chicago, 1965.